Available online at www.sciencedirect.com
SCIENCE DIRECT
Cement and Concrete Research 35 (2005) 2310–2321
Cement and Concrete Research

The kinetics of ettringite formation and dilatation in a blended cement with β-hemihydrate and anhydrite as calcium sulfate

Cecilie Evju[a,*], Staffan Hansen[b]

[a]Optiroc AS, P.O. Box 216 Alnabru, N-0614 Oslo, Norway
[b]Materials Chemistry, Center for Chemistry and Chemical Engineering, Lund University, P.O. Box 124, S-221 00 Lund, Sweden

Received 23 September 2003; accepted 14 September 2004

Abstract

The phase formation, heat of hydration and dilatation in a blended cement consisting of 50 wt.% calcium aluminate cement, 25 wt.% Portland cement and 25 wt.% calcium sulfate were studied (w/c=1). The calcium sulfate was β-hemihydrate, anhydrite and mixes of the two. Kinetic expressions describing the ettringite formation in the pastes with the pure calcium sulfates were found. Hydration reactions were suggested and the phase development was compared to the hydration heat by mass and heat balances. When the calcium sulfate was 75 and 50 wt.% β-hemihydrate, the systems behaved as a linear combination of the 100 and 0 wt.% blends. At 25 wt.%, the hydration kinetics differed from the other blends. With only β-hemihydrate, the last 50% of ettringite formation was accompanied by expansion, mainly caused by interaction of crystals growing radially on cement grains. In the paste with only anhydrite, ettringite crystals grew in solution and produced no expansion.

Keywords: Hydration; Kinetics; Thermodynamic calculations; Expansion; Ettringite

1. Introduction

Ettringite forms during hydration of various inorganic binders. In cement chemistry, ettringite formation is combined with both problems and beneficial properties. The expansion in several expansive or shrinkage compensating cements is associated with ettringite formation [1]. The major aluminate phases responsible for the formation of ettringite varies with the cement type, it is $C_4A_3\hat{S}$ in Type K cement, CA in Type M, and C_3A in Type S [1]. The mechanism concerning ettringite formation and expansion has been investigated for decades, and is still not fully understood. The numerous investigations concerning ettringite formation and cement expansion can be divided into two schools: (i) the crystal growth theory and (ii) the swelling theory [1]. Several studies supports both schools, a few of them are summarised here. The basis of the crystal growth theory is that the ettringite crystals grow on the surface on the cement particles and the growth of the crystals gives rise to a crystallisation pressure and hence to an expansion. Ogawa and Roy [2] found that ettringite first formed small and irregular crystals around the $C_4A_3\hat{S}$ particles. As the hydration continued, the ettringite crystals became radially arranged around the cement grains and the expansion began when the reaction zones came in contact with each other. Bentur and Ish-Shalom [3,4] assumed ettringite formation on spherical $C_4A_3\hat{S}$ particles and showed that the expansion did not start until a critical degree of hydration was obtained and a first contact is formed between the expanding spheres. The swelling theory was introduced by Mehta [5] who suggested the formation of ettringite crystals to have a through-solution mechanism and that the dissolution of the aluminates was decreased by the presence of lime, which caused the ettringite to be colloidal in size and be gel-like. On the resulting large

* Corresponding author.
E-mail address: cecilie.evju@optiroc.no (C. Evju).

0008-8846/$ - see front matter © 2004 Elsevier Ltd. All rights reserved.
doi:10.1016/j.cemconres.2004.09.012

surface of ettringite, water can be absorbed and that will lead to an overall expansion of the system. In the absence of lime, the aluminate phase will react rapidly and form long ettringite crystals, which will not produce any expansion because of their small surface area. Mehta and Wang [6] supported the theory by showing that blends with smaller ettringite crystals expanded considerably more than blends with larger crystals. Deng and Tang [7] concluded that expansion is a combination of both crystallisation pressure generated by ettringite growth and by swelling caused by selective absorption of ions with a large amount of water on tiny ettringite crystals. They also concluded that, in order to grow ettringite crystals, which gave expansion a high alkalinity was necessary, low alkalinity gave coarse ettringite crystals which caused little or no expansion.

The studies on the kinetics of ettringite formation mainly concern the formation from pure phases and gypsum [8]. The kinetic expression utilised is not always suitable to describe the formation of ettringite in expansive cements. Kinetic analysis has been preformed in several in situ studies of zeolite crystallisation with synchrotron X-ray diffraction [9,10]. The most commonly used kinetic model is the Avrami equation (Eq. (1)). Eq. (1) describes the degree of formation of the product, α, as a function of time, t. The parameter n in Eq. (1) is empirically related to different nucleation and growth mechanisms in solid-state reactions [11] and k_1 is the crystal growth rate constant. The Avrami equation is originally a model to describe solid–solid phase transformation [11]. Although it is valid only for solid-state reactions and not for solution-mediated processes, it has been used with some success to describe the growth kinetics of zeolites and it may be applicable to the description of phase formation during cement hydration because neither of these systems have any long-range transport of material.

$$\alpha = 1 - \exp(-k_1 t)^n \quad (1)$$

Recently, another model developed to extract kinetic data from X-ray diffraction experiments was presented [12]. In addition to the crystal growth described by Eq. (1), it includes a description of the nucleation process, cf. Eq. (2). In Eq. (2), the parameter n has a strict meaning as it refers to the crystal growth dimension (1=needles, 2=plates, 3=spheres). The nucleation rate constant, k_n, can be derived from the parameter a, $k_n=1/a$, and b refers to the whether the nucleation mechanism is heterogeneous ($b \leq 900$ sec), homogenous ($b \approx 1200$ sec), or autocatalytic ($b>1200$ sec) [12] and k_2 is the crystal growth rate constant.

$$\alpha = \frac{1}{1 + \exp\left(-\frac{t-a}{b}\right)}\left[1 - \exp(-k_2 t)^n\right] \quad (2)$$

Synchrotron X-ray diffraction identifies the crystalline reaction products and gives the opportunity to follow their formation over time, but the availability of the technique is so far limited. Isothermal calorimetry gives the total heat development as a function of time; it has a simple experimental procedure and better availability than synchrotron radiation. By using the phase development to suggest reactions and combining these with thermodynamic data, the results from the two methods can be compared. This is useful for checking whether the suggested reactions are reasonable and whether there are reactions with only amorphous hydration products. It may also open possibilities for a better interpretation of results on hydration heats on similar systems when synchrotron radiation is not available.

The alumina-bearing cement paste has been recognised as an important factor concerning the overall expansion, as well as the kinetics of ettringite formation and expansive properties of ettringite [13,14]. The influence of the type of calcium sulfate is far less investigated. In pastes with calcium aluminate cement and calcium sulfate, it has been shown that gypsum gives a faster ettringite formation compared to anhydrite and that both systems are accelerated by small additions of lime [15,16]. The difference was explained in the varying supersaturation caused by the difference in sulfate release to solution and only the pastes with gypsum showed expansion [15]. Previous studies have shown that a blended cement consisting of calcium aluminate cement, Portland cement, and β-calcium sulfate hemihydrate forms ettringite as the major early hydration product and the formation of ettringite is associated with expansion [17]. In this study, the calcium sulfate has been β-hemihydrate, anhydrite, and mixes of the two in the same blended cement. The phase development has been followed by synchrotron X-ray diffraction, the heat of hydration followed by isothermal calorimetry, and the dilatation of the pastes measured. The kinetics of ettringite formation has been studied and hydration reactions has been proposed and compared, in combination with thermodynamic data, to the measured heat of hydration. The microstructure of hydrated samples has been investigated and a connection between ettringite formation and expansion proposed.

2. Experimental

2.1. Cements and data collection

The cement blends examined consisted of 50 wt.% calcium aluminate cement, 25 wt.% ordinary Portland cement, and 25 wt.% calcium sulfate. Water to solid ratio of unity was utilized. The major phases in the calcium aluminate cement were CA, C_4AF, and $C_{12}A_7$. The calcium sulfate was β-hemihydrate, anhydrite, or mixes of the two. The compositions of the five pastes studied are specified in Table 1. All cementitious materials were commercially available products and both calcium sulfates were contami-

Table 1
The calcium sulfate compositions in the five pastes studied

Paste no.	wt.% β-hemihydrate	Percent (%) anhydrite
1	100	0
2	75	25
3	50	50
4	25	75
5	0	100

The cement contained 50 wt.% calcium aluminate cement, 25 wt.% Portland cement, and 25 wt.% calcium sulfate. The water to solid ratio was equal to unity.

nated by a few weight percent of gypsum. The Portland cement and the calcium aluminate cement have similar grain size distribution and all the grains are smaller than 90 μm. The anhydrite has somewhat coarser grains, but a size distribution curve of similar shape as the cements and all the grains are smaller than 106 μm. The β-hemihydrate differs, with larger grains than the other raw materials, only 70% is smaller than 90 μm and the largest grains are 500 μm. The experiments were preformed at room temperature and at 100% relative humidity.

The dilatation of the pastes was measured as described earlier [17]. Three measurements on each paste were performed and the average is presented here. The heat of hydration was followed by an isothermal calorimeter. The experiments were performed according to Ref. [17] and the data were dynamically corrected with two time constants as outlined elsewhere [18]. The average of three measurements is presented here. The phase formation during hydration was followed by synchrotron X-ray powder diffraction on beamline I711 at MAX-lab in Lund, Sweden. Experiments were performed on several occasions with monochromatic radiation of wavelengths around 1.5 Å. On one occasion, the wavelength was 1.1 Å. Sample preparation and data evaluation were done as previously described [17]. The data were collected using either a Bruker system with a SMART 1000 CCD detector, a Huber Guinier image foil camera 670, or a Marresearch 165 mm CDD detector mounted on a Marresearch Desktop Beamline baseplate. When using the SMART detector, each spectrum was collected for a total of 3 min; when the Guinier camera was used, the spectra were collected for 6 min each; and when the Marresearch detector was used, the spectra were collected for just over 7 min each. The total time for each data collection varied between 7 and 12 hours. The peak intensities calculated were corrected for the decay in beam intensity during the experiments. The relative peak intensities were used to monitor the degree of formation and dissolution (α) of a phase as a function of time (t). For investigation of the microstructure by scanning electron microscopy (SEM), pastes were prepared by mixing cement and water with a blender, poured on a plastic surface, and covered with another to ensure 100% relative humidity. To stop the hydration, the samples were rinsed with acetone (Merck, >99.5%) under vacuum filtration. The samples was sputtered with gold and examined by secondary electron imaging in a JSM-840A scanning electron microscope.

2.2. Kinetic analysis

The kinetic parameters in Eqs. (1) and (2) were obtained by using least square fittings to the experimental data on ettringite formation in pastes 1 and 5, in order to investigate whether the equations were able do give a good description of the ettringite formation. Kinetic expressions describing the ettringite formation in pastes 1 and 5 were found, $\alpha_1(t)$ and $\alpha_5(t)$, respectively. The remaining three pastes can be considered to be mixes of the two pure pastes (1 and 5; Table 1). Ettringite is the common hydration product so the two systems influence on each other's hydration kinetics, i.e., ettringite formation, is of interest. There are three possibilities for the reaction kinetics of pastes with mixed sulfates.

(i) They react as two isolated systems and their ettringite formation can be described as a linear combination of the ettringite formations in pastes 1 and 5, as described by Eq. (3), where γ describes the weight fraction of paste 1 in the mixed paste (or the weight fraction of β-hemihydrate in the calcium sulfate in the paste).
(ii) They follow the same kinetic expressions as the pure pastes but they influence each others kinetic parameters.
(iii) A completely new kinetic expression is necessary.

To investigate which of the three alternatives was valid, (i) the linear combination from Eq. (3) was calculated and (ii) the kinetic parameters in the expressions for α_1 and α_5 were allowed to change. The calculated curves were compared to the experimental data from synchrotron X-ray diffraction.

$$\alpha_{\mathrm{mix}} = \gamma\alpha_1 + (1-\gamma)\alpha_5 \tag{3}$$

The hydration kinetics in the pastes can also be studied by isothermal calorimetry. By integration of the calorimeter output, the heat of hydration for the reactions is obtained. This will take into account all reactions taking place in each paste, not only the ettringite formation. To further investigate the connection between the hydration kinetics in pastes 1 and 5 and in the mixes of the two, the hydration curves for pastes 2–4 (Q_{mix}) were calculated by Eq. (4) and compared to the experimentally measured heats of hydration.

$$Q_{\mathrm{mix}} = \gamma Q_1 + (1-\gamma)Q_5 \tag{4}$$

The parameter γ is still the weight fraction of β-hemihydrate (or fraction of paste 1) and Q_1 and Q_5 are the measured heat of hydration for pastes 1 and 5, respectively.

2.3. Mass and heat balances

Based on the identified hydration products and degrees of reaction (α) from X-ray diffraction, possible reactions and mass balances for paste 1 were suggested. The calcium aluminate cement was approximated as pure CA and the Portland cement as C_3S. From the first reactions and mass balances, a value for the heat of formation of the C–S–H gel was calculated. The calculated heat from the assumed reactions and their reaction enthalpies were compared to the calorimetric data. With the acquired thermodynamic data from the calculations on paste 1, a reaction was proposed for the ettringite formation in paste 5 and the X-ray and calorimetric data were compared.

3. Results and discussion

3.1. Phase development

A thorough description of the phase development in the paste 1 (100 wt.% β-hemihydrate) has been given earlier [17]. Gypsum is formed from β-hemihydrate during the first 30 min of hydration; ettringite starts to form during the first 10 min and continues to form until all the gypsum is consumed after about 4 hours (Fig. 1). When the calcium sulfate is consumed, the calcium aluminate cement continues to react with water and forms C_2AH_8 (aluminate-AFm). In paste 5 (100 wt.% anhydrite), the only hydration product detected by X-ray powder diffraction is ettringite. The amount of ettringite increases slowly for the first 2 hours when a faster growth starts and the formation of ettringite continues throughout the experiment, totally about 12 hours (Fig. 2).

In pastes 2 and 3, gypsum and ettringite are identified as the hydration products. Gypsum is consumed during the same period of time as in the paste with only β-hemihydrate,

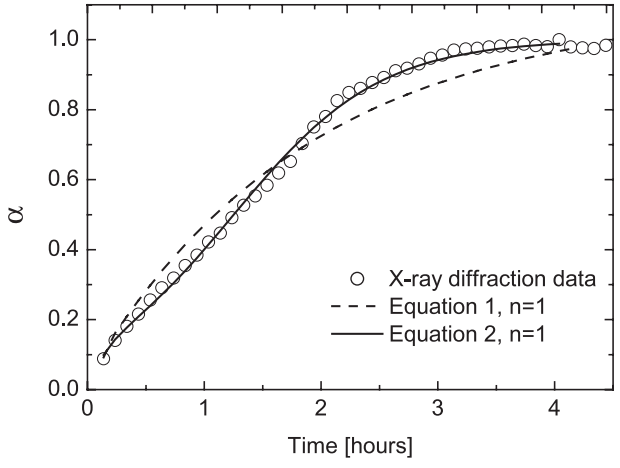

Fig. 1. Paste with 100 wt.% β-hemihydrate (paste 1); Ettringite formation from X-ray diffraction (○) [17] and kinetic analysis according to Eqs. (1) and (2).

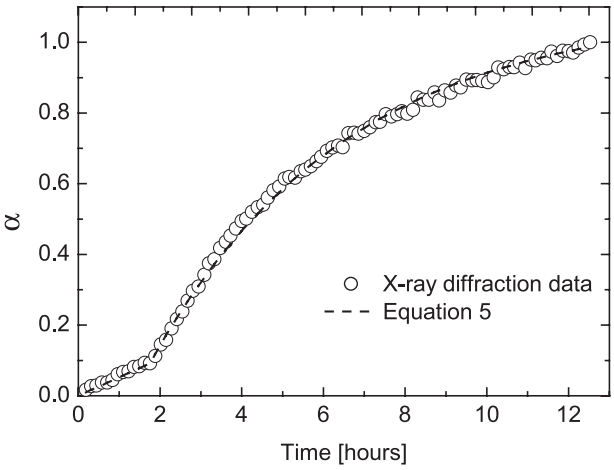

Fig. 2. Paste with 100 wt.% anhydrite (paste 5); Ettringite formation from X-ray diffraction (○) and kinetic analysis according to Eq. (5).

but the initial gypsum consumption is faster in pastes 2 and 3 (Fig. 3). The gypsum formation from β-hemihydrate is faster in paste 2 than in paste 1. In pastes 2 and 3, ettringite appears to grow in two steps, one fast and one slow. In the two mixes, the ettringite crystallisation was ongoing at the end of the experiment, after approximately 10 hours. The ettringite formation for pastes 2 and 3 is shown in Fig. 4. Fig. 4 shows that the ettringite formation in pastes 2 and 3 are divided into two parts. The first part coincides well in time with the consumption of gypsum (Fig. 3) and the relative amount of ettringite formed during this period of time fits well with the fraction of β-hemihydrate in the pastes (horizontal line in Fig. 4). The fraction of ettringite formed after the consumption of gypsum does coincide with the fraction of anhydrite. As a consequence, it can be concluded that (i) only a very small part of the anhydrite can dissolve during the first part of the reaction, (ii) the reactions are almost completed at the end of the experiments, and that (iii) only a small fraction of the anhydrite is insoluble. If a considerable amount of anhydrite was not reacted at the end of the experiment, the amount of ettringite formed after gypsum was consumed would be smaller than the relative

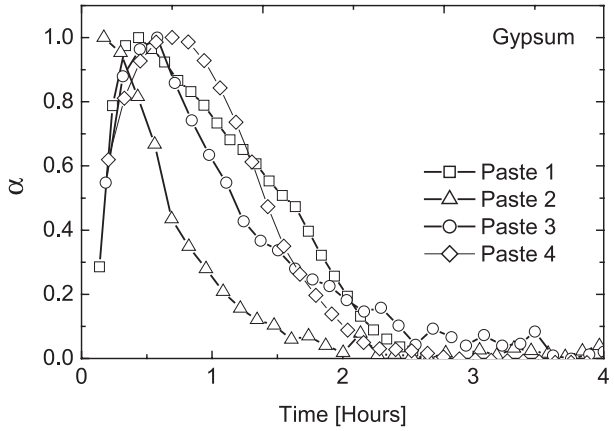

Fig. 3. The relative amount of gypsum as a function of time in pastes 1 (□), 2 (△), 3 (○), and 4 (◇) data for paste 1 published in Ref. [17]).

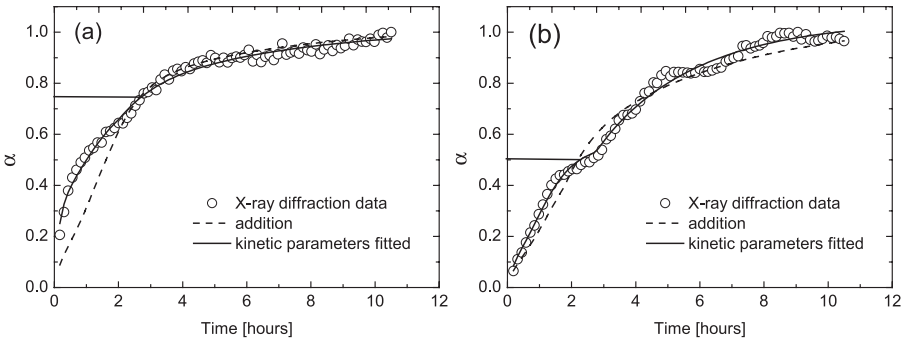

Fig. 4. The ettringite formation in (a) paste 2 (75 wt.% β-hemihydrate) and (b) paste 3 (50 wt.% β-hemihydrate). (○) Experimental data from X-ray diffraction; (- - -) linear addition of the ettringite formation rates in pastes 1 and 5 according to Eq. (3); (—) addition with the kinetic parameters fitted to the experimental data according to Table 2. The horizontal lines show the relative amounts of β-hemihydrate in the calcium sulfate.

amount of anhydrite, and the fraction of ettringite formed in the early reaction would consequently exceed the fraction of β-hemihydrate in the paste.

Paste 4 (25 wt.% β-hemihydrate) shows a phase development which diverges from the other pastes (Fig. 5). The β-hemihydrate dissolves during the first hour of hydration, while gypsum forms and ettringite does also form rapidly during this period of time. During the next 2 hours of hydration, gypsum is consumed and ettringite continues to form. When all the gypsum is consumed, the ettringite formation rate is highly reduced; the relative amount of ettringite increases slowly from 3 to 4 hours of hydration to the end of the experiment. When the gypsum was consumed, a new phase started to form. It was identified as sulfate AFm ($C_4A\hat{S}H_{12}$), normally denoted monosulfate in cement chemistry and known from Portland cement hydration. Monosulfate was not found in any of the other pastes. At the end of the experiment, the monosulfate peak was still small; the intensity was less than 5% of the main ettringite peak. The utilised detector in this experiment, the Marresearch CCD, gives a lower noise in the background compared to the other two detectors. As it has only been utilised in one experiment,

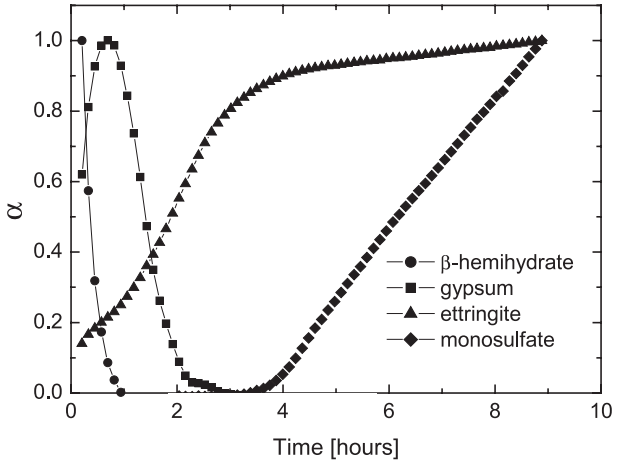

Fig. 5. The phase development measured with synchrotron X-ray diffraction in paste 4.

the hydration of paste 4, it is possible that the reflections from monosulfate are not reaching above the background noise in the other experiments. The reason for monosulfate formation may be the slow dissolution of the anhydrite. If the Portland cement and calcium aluminate cement dissolves faster than anhydrite with reference to ettringite formation, the solution may become supersaturated in another solid substance. Ettringite and monosulfate will need the same relative amount of calcium and aluminium from cement, but ettringite needs three times the calcium sulfate compared to monosulfate in order to form. The depletion of anhydrite is difficult to quantify by X-ray diffraction. Mainly because in the studied mixtures, no singular anhydrite peak is available, they all overlap with reflections from other phases present in the system. The main anhydrite peak at d=3.499 Å overlaps with a minor ettringite peak. Because the SMART and Marresearch CCD detectors collect two-dimensional ring patterns, they give the opportunity to follow the changes in the anhydrite content, although it is hard to get any quantitative information. Fig. 6 shows the ring at d=3.499 Å at three different occasions during the hydration of paste 4. The large grains of anhydrite do not appear to dissolve at all and are visible in the later two diffraction patterns as distinct dots. Fig. 6b shows the anhydrite ring after 4 hours of hydration; that is, after the gypsum is consumed. It is visible that substantial amounts of anhydrite has dissolved during the hydration so far; that is, the solid bright line at the start of the experiment (Fig. 6a) has become less bright and contains dots. During the last 5 hours of hydration, there is a slight reduction in the intensity of the ring, corresponding to the formation of monosulfate and ettringite. The reduction in anhydrite intensity in Fig. 6b shows that the ettringite formed during the first hours of hydration, when gypsum formed and was consumed, is not only the product of the initial β-hemihydrate but also that the anhydrite dissolves simultaneously and delivers sulfate to ettringite and possibly to gypsum. The reflections from ettringite are high compared to the cement peaks, also indicating more ettringite than from the 25 wt.% of β-hemihydrate in the sample. Consequently, paste 5 diverts from the other two mixes, pastes 2 and 3, by having substantial anhydrite dissolution and consequent

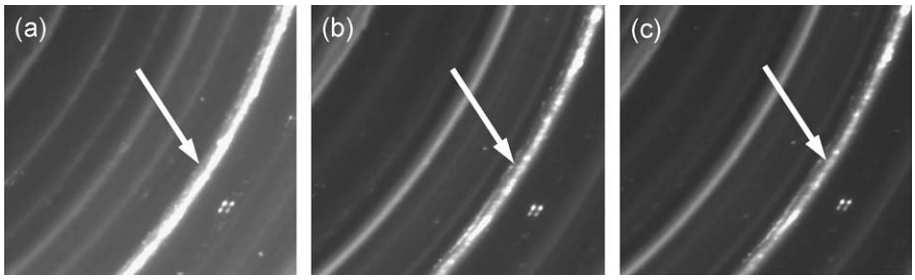

Fig. 6. The strongest anhydrite diffraction ring (marked by arrow) in the (a) first diffractogram (12 min), (b) after about 4 hours (when the monosulfate starts to form), and at the (c) last measurement (9 hours) in a data series measured with X-ray synchrotron diffraction on paste 4. The anhydrite ring overlaps with a minor one from ettringite.

ettringite formation during the β-hemihydrate-related reactions. A similar study of the anhydrite reflection is not possible in the data from the paste 2 and 3 hydrations because these were collected with the Huber Guinier detector which gives a one-dimensional X-ray spectrum. The intensity of the peak is highly dependent on the amount of big grains of anhydrite in the irradiated area of the sample, a parameter impossible to evaluate with normal powder X-ray diffraction.

When performing phase formation experiments with synchrotron X-ray diffraction, the sample that is studied is very small. Large grains can block parts of the capillary and produce inhomogeneous zones inside the capillary when the paste is drawn inside. This problem is minimised by first drawing a large proportion of the prepared sample into the capillary and syringe, and then a part of the paste in the syringe is pushed out through the capillary. The beam hitting the sample is approximately 1 mm×1 mm; a very small fraction of the prepared sample is irradiated. Because of this, there will be a possibility that the composition of the irradiated sample is not completely similar to the prepared bulk sample. Apparently, the largest anhydrite crystals do not dissolve at all during the experiments (Fig. 6c).

When ordinary Portland cement hydrates alone, the silicate phases form $Ca(OH)_2$ in addition to C–S–H gel [19]. When Portland cement is mixed with calcium aluminate cement in small amounts, the same hydration phases are observed as in ordinary Portland cement. When the major part is calcium aluminate cement, no $Ca(OH)_2$, ettringite, or other Portland cement hydration products have been discovered by X-ray diffraction in previous studies [20,21], only calcium aluminate cement hydration products as CAH_{10} and C_2AH_8. In this study, no evidence for $Ca(OH)_2$ formation was found from X-ray diffraction, which agrees well with the previous studies.

3.2. Kinetic analysis

Fig. 1 shows that using n=1 for needle-formed crystals, the ettringite crystallisation in paste 1 (100 wt.% β-hemihydrate) can be described by Eq. (2). The kinetic parameters obtained by least square fitting are listed in Table 2. As b>1200 sec, the nucleation is autocatalytic. By using Eq. (1), it was not possible to properly describe the ettringite formation rate from the X-ray diffraction data for paste 1 (Fig. 1) for any value of n. The slow ettringite growth during the first 2 hours of hydration in paste 5 (100 wt.% anhydrite, Fig. 2), i.e., an induction period, was not possible to model by neither Eq. (1) nor Eq. (2). The kinetic expression was therefore divided into two, the induction and the crystal growth periods as described by Eq. (5).

$$\begin{aligned} \alpha &= \tfrac{\alpha_0}{t_0} t && \text{when } t<t_0 \\ \alpha &= \alpha_0 + [1-\exp(-k_1(t-t_0))] && \text{when } t\geq t_0 \end{aligned} \quad (5)$$

α_0 is $\alpha(t_0)$ and was determined from the experimental data. When using Eq. (2) as the second half of Eq. (5) (for $t\geq t_0$), the values of parameters a and b were found to be insignificant to the least square fitting result. The shape of the experimental curve made only the crystal growth part of the equation important. As a consequence, Eq. (1) was used with the parameter n=1, which, for cylindrically shaped crystals, implies diffusion controlled growth. This interpretation refers to solid-state processes [11] and should not be considered significant in this case. The fitted curve is shown in Fig. 2 and the kinetic parameters are listed in Table 2. The Avrami equation, as expressed in Eq. (1), will reach from 0 to 1; that is, it is equal to 1 when the formation is completed or at the end of the experimental data as the experimental data are normalised to a relative amount and will also reach from 0 to 1. The crystal growth rate constant, k_1, obtained by fitting will therefore be highly dependent on how far the ettringite formation in an experiment is from reaching the end, i.e., when the relative intensity should be one. Consequently, k_1 will depend on for how long an experiment is performed. An explanation to the apparent insignificance of the nucleation part of Eq. (2) may be that,

Table 2
The kinetic parameters from least squares fitting for pastes 1 (Eq. (2), $\alpha 1$) and 5 (Eq. (5), α_5)

Paste no.	a [s]	b [s]	k_2 [s^{-1}]	t_0 [s]	k_1 [s^{-1}]
1	4509	2255	2.35×10^{-3}		
5				6320	5.51×10^{-5}
2	3276	1938		9941	8.85×10^{-5}
3	1507	3345		7214	5.35×10^{-5}

For pastes 2 and 3, the adjusted parameters in α_1 and α_5 are given for least square fitting of the combinations of α_1 and α_5 according to Eq. (3).

during the induction period (or slow crystallization), up to $t=t_0$, a supersaturation builds up in the solution and numerous nuclei are formed and after $t=t_0$, crystallization continues on these nuclei.

The linear addition of the kinetic expressions describing ettringite formation in pastes 1 and 5 according to Eq. (3) for $\gamma=0.75$ and $\gamma=0.50$, i.e., pastes 2 and 3, are shown in Fig. 4. The simple addition of the kinetic expressions for pastes 1 and 5 comes close to describing the kinetics of ettringite formation in the mixed pastes. Apparently, the fast part of the ettringite formation, caused by the β-hemihydrate, is faster in the mixes than it is when only β-hemihydrate is present (paste 1). The kinetic parameters in α_1 and α_5 were consequently investigated; the values from least square fitting are shown in Table 2. In the β-hemihydrate expression (α_1), the crystal growth was found to be constant in all mixes, but the nucleation rate ($1/a$) was larger in the mixes than in the pure paste (paste 1). The nucleation mechanism was not influenced. In the anhydrite expression (α_5), t_0 increased significantly in the mixes compared to the paste with only anhydrite (paste 5). The crystal growth rate does change, but it is difficult to make any interpretations of this as the experimental data are normalised and thus reaches from 0 to 1 although the ettringite formation is still ongoing at the end of the experiments. The rate constant is therefore dependent on the difference between t_0 and the time at the end of the experiment, as Eq. (5) will make it reach between α_0 and 1 in this period of time, independent on how far the ettringite formation really is from reaching the end. The kinetic parameters for pastes 2 and 3 are listed in Table 2 and the fitted curves are also shown in Fig. 4. The results show that, when paste 1 and paste 5 are mixed, the ettringite formation in the mixed paste will be a linear combination of the ettringite formation in the pure systems down to a β-hemihydrate content of 50 wt.%, but their kinetic parameters are influenced by the presence of the other system. When water is added to the cement mixes, crystal growth starts immediately in the β-hemihydrate system, while in the anhydrite system, the major crystallization appears to have an induction period. The increased nucleation rate in the β-hemihydrate system in the mixed pastes may be explained by some dissolution of anhydrite, which then contributes to ettringite nucleation. It can also be caused by dissolution of the gypsum contaminating anhydrite. Because the initial ettringite crystal growth is much stronger in the β-hemihydrate system, the ettringite formed from β-hemihydrate grows on all available nuclei present until all the β-hemihydrate and gypsum is consumed and the sulfate incorporated in ettringite. The crystallization due to anhydrite starts when the β-hemihydrate-based reaction is ended. Apparently, the faster reaction uses all available crystallisation sites, so the slower reaction cannot compete for these and thus has to wait for them to be available before it starts.

The ettringite formation in paste 4 is not possible to be described by Eq. (3) because it appears to react differently with pastes 2 and 3. Ettringite forms mainly during the consumption of β-hemihydrate and gypsum (Fig. 5). When the gypsum is consumed, monosulfate forms in addition to ettringite, and the ettringite formation is slower than during the gypsum consumption (Fig. 5). It does also appear that a larger amount of the anhydrite dissolved during these early reactions in paste 4 compared to pastes 2 and 3.

The influence of small sample sizes in synchrotron X-ray diffraction has already been discussed. The small sample size and the possible inhomogeneities may influence the crystallisation because the number of possible crystallisation sites may vary in the sample. A study of gypsum formation from β-hemihydrate with synchrotron diffraction [22] showed variations up to approximately 10% in identical experiments, even when gypsum crystals were added to facilitate nucleation. The kinetic parameters are therefore only indications on the reactivities and do not give full descriptions of the systems.

The measured heats of hydration by calorimeter for pastes 1–5 are given in Fig. 7 together with the calculated heats of hydration for pastes 2–4 according to Eq. (4). The experimental curves for pastes 2 and 3 are both increasing faster than the calculated curves during the first hours, indicating that the fast initial reactions of paste 1 are accelerated by the presence of paste 5. At approximately 12 hours, the calculated curves exceed the measured ones. The latter reactions are thus slower in the mixes than in the pure pastes. When hydration material builds up, it may slow down the following rate of hydration because the diffusion length for dissolved ions increase if the hydration products form on the surface of the cement. In paste 4 (25 wt.% β-hemihydrate), there also appears to be a slight acceleration of the earliest reaction (the first 2 hours). As opposed to pastes 2 and 3, the reactions after 3 hours of hydration are also faster in the mixture than in the pure paste (Fig. 7d). All three mixed pastes (2–4) show an increased hydration heat between 4 and 12 hours of hydration compared to the calculated heat from Eq. (4); the deviation increases with the amount of anhydrite in the paste. In paste 4, monosulfate starts to form after 4 hours of hydration. The increased heat of hydration may be caused by formation of monosulfate in all mixed pastes and indicates that the phase only is present when the calcium sulfates are utilised together.

3.3. Mass and heat balances

3.3.1. Paste 1

The thermodynamic data utilised for calculation and references to literature are given in Table 3.

The hydration of paste 1 (100 wt.% β-hemihydrate) can be divided into different time periods, all limited by the reactions taking place during the given period of time.

3.3.2. $t=0-t_1$, consumption of β-hemihydrate

During the consumption of β-hemihydrate, gypsum and ettringite are forming. Gypsum formation from β-hemi-

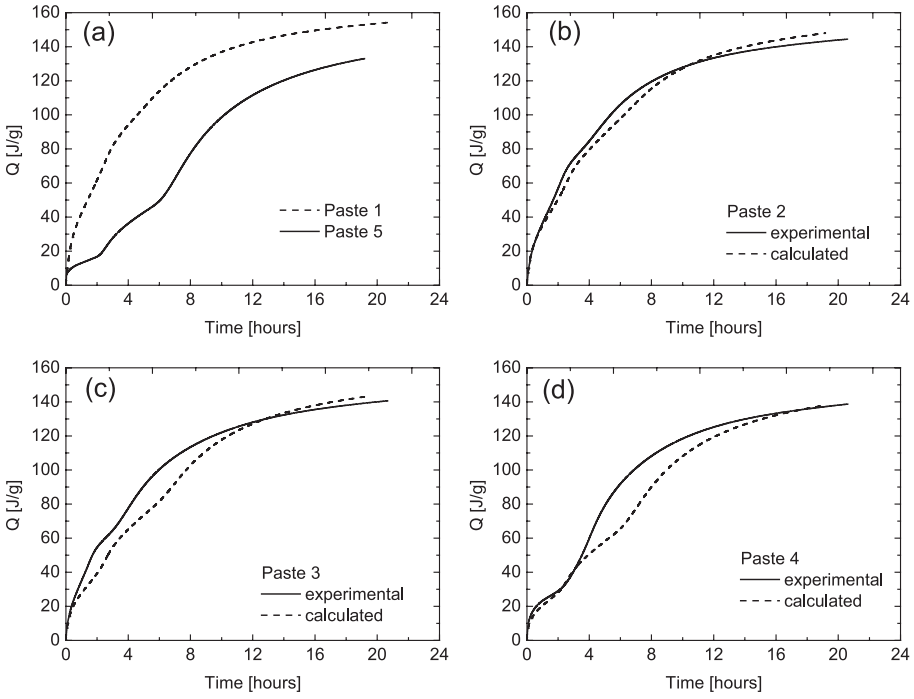

Fig. 7. The heat of hydration measured by calorimeter (a) Experimental curves for pastes 1 and 5. The experimental (—) and calculated curves (Eq. (4)) (- - -) for (b) paste 2 (c) paste 3, and (d) paste 4.

hydrate is described by Reaction 1. The calcium aluminate cement is represented as pure CA and Portland cement as pure C_3S. The composition of the C–S–H gel is normalised to $C_3S_2H_4$ for simplicity. This composition is not far from experimentally determined compositions [19]. The ettringite formation during the consumption of hemihydrate can then be expressed by Reaction 2. The phases CA and β-hemihydrate are deficient in calcium, compared to aluminium and sulfate, in order to form ettringite on its own, so the dissolution of Portland cement is necessary to balance the reaction. Portland cement, on its hand, contributes its excess calcium to ettringite instead of forming $Ca(OH)_2$, a reasonable assumption because no $Ca(OH)_2$ has been observed in the X-ray diffraction experiments. The time t_1 can be found from X-ray diffraction data; that is, when all the β-hemihydrate is consumed. The amount of β-hemihydrate in the paste is limiting the reactions and the mass balances for this period of time are given by Eq. (6)

Table 3
The enthalpy of formation utilised in calculation and reference to literature

Phase	ΔH_{298} [kJ mol^{-1}]	Reference
CA	−2326	[23]
C_3S	−2928	[19]
$CaSO_4$	−1434	[24]
$CaSO_4 \cdot 1/2H_2O$	−1577	[24]
$CaSO_4 \cdot 2H_2O$	−2023	[24]
$C_6A\hat{S}_3H_{32}$	−17,539	[19]
C_2AH_8	−5435.9	[25]
AH_3	−1276	[24]
H_2O (l)	−286	[24]

(assuming no substitutions of other ions for sulfate in ettringite). The amount of gypsum and ettringite at $t=t_1$ can be calculated from the X-ray diffraction data. Because $n_{CSH0.5}$(start) is known, and the heat produced during the time period is described by Eq. (7), expressed by the reaction enthalpies and the degree of reaction in Reactions 1 (α_{11}) and 2, where α_{21} is the total rate of formation for ettringite from synchrotron X-ray diffraction.

$$\text{(Reaction1)}\quad CaSO_4 \cdot 1/2H_2O + 3/2H_2O \rightarrow CaSO_4 \cdot 2H_2O$$

$$\text{(Reaction2)}\quad 199/6H + CA + 3C\hat{S}H_{0.5} + 4/3C_3S \rightarrow C_6A\hat{S}_3H_{32} + 2/3C_3S_2H_4$$

$$n_{C\hat{S}H_{0.5}}(\text{start}) = n_{C\hat{S}H_{0.5}}(t) + n_{C\hat{S}H_2}(t) + 3n_{C_6A\hat{S}_3H_{32}}(t) = n_{C\hat{S}H_2}(t_1) + 3n_{C_6A\hat{S}_3H_{32}}(t_1) \quad (6)$$

$$Q_1(t) = \alpha_{11}(t)n_{C\bar{S}H_2}(t_1)\Delta H_1 + \alpha_{21}(t)n_{C_6A\bar{S}_3H_{32}}(\max)\Delta H_2 \quad (7)$$

3.3.3. $t=t_1-t_2$, consumption of gypsum, formation of ettringite

Reaction 3 describes the formation of ettringite while gypsum it consumed. It is similar to Reaction 2. The ettringite formation is limited by the amount of sulfate, i.e., by the amount of β-hemihydrate in the cement blend (assuming that no other sulfate phases are formed) (Eq. (8)).

The heat produced by Reaction 3 (q_3) can be expressed by the reaction enthalpy and reaction parameter (α_3) (Eq. (9)). Substituting α_3 with the total ettringite formation, α_{21}, the accumulated heat production in this period of time will be expressed by Eq. (10).

$$\text{Reaction3}\quad 86/3\text{H} + \text{CA} + 3\text{C}\hat{\text{S}}\text{H}_2 + 4/3\text{C}_3\text{S} \rightarrow \text{C}_6\text{A}\hat{\text{S}}_3\text{H}_{32} + 2/3\text{C}_3\text{S}_2\text{H}_4$$

$$n_{\text{C}_6\text{A}\hat{\text{S}}_3\text{H}_{32}}(t_2) = n_{\text{C}_6\text{A}\hat{\text{S}}_3\text{H}_{32}}(\max) = 1/3 n_{\text{C}\hat{\text{S}}\text{H}_{0.5}}(\text{start}) \tag{8}$$

$$q_3(t) = \alpha_3(t)\left(n_{\text{C}_6\text{A}\bar{\text{S}}_3\text{H}_{32}}(\max) - n_{\text{C}_6\text{A}\bar{\text{S}}_3\text{H}_{32}}(t_1)\right)\Delta\text{H}_3 \tag{9}$$

$$Q_3(t) = Q_1(t_1) + (\alpha_{21}(t) - \alpha_{21}(t_1)) n_{\text{C}_6\text{A}\bar{\text{S}}_3\text{H}_{32}}(\max)\Delta\text{H}_3 \tag{10}$$

Fig. 8 shows the connection between the calorimetric data for paste 1 and Eqs. (7) and (10). The enthalpy of formation for $C_3S_2H_4$ was fitted to scale the experiments up to t_2 and found to be $\Delta H_f(C_3S_2H_4)$=−4762 kJ/mol. The enthalpy of formation for tobemorite ($C_3S_2H_2$) with excess hydration water and a specific surface of 300 m^2/g is −4793 kJ/mol [25]. The value is dependent on the specific surface and the amount of adsorbed water. The obtained value is thus reasonable. The calorimetric data and X-ray diffraction data coincide well in shape, indicating that there are no additional reactions with only amorphous hydration products taking place during the ettringite formation ($t<t_2$). The reasonable value for the heat of formation of the C–S–H gel indicates that the suggested reactions are a suitable description of the ongoing hydration in the system.

3.3.4. $t=t_2-t_3$, formation of C_2AH_8

When all the sulfate is incorporated in ettringite, C_2AH_8 is the consecutive crystalline hydration phase, and the formation can be expressed by Reaction 4. Again, C_3S provides calcium to the hydration product from the calcium aluminate cement and, as a consequence, only C–S–H gel is formed, no $Ca(OH)_2$. The limitation for Reaction 4 is the amount of C_3S. When there is no C_3S left, Reaction 5 is reasonable to assume as the next step. Because the amount of C_3S is limiting Reaction 4, it is practical to refer α_4 and ΔH_4 to the amount of $C_3S_2H_4$ formed in Reaction 4 ($\Delta H_4'$=3ΔH_4). The relationship between C_3S and $C_3S_2H_4$ is n_{C_3S}(start)=2$n_{C_3S_2H_4}$(max); consequently, the heat formed from Reaction 4 can be expressed by Eq. (11) and the accumulated heat in this period of time will be described by Eq. (12).

$$\text{Reaction4}\quad 28/3\text{H} + \text{CA} + 2/3\text{C}_3\text{S} \rightarrow \text{C}_2\text{AH}_8 + 1/3\text{C}_3\text{S}_2\text{H}_4$$

$$\text{Reaction5}\quad 11\text{H} + 2\text{CA} \rightarrow \text{C}_2\text{AH}_8 + \text{AH}_3$$

$$q_4(t) = \alpha_4(t) n_{\text{C}_3\text{S}_2\text{H}_4}(\max)\Delta\text{H}_4' = 1/2\alpha_4(t) n_{\text{C}_3\text{S}}(\text{start})\Delta\text{H}_4' \tag{11}$$

$$Q_4(t) = Q_3(t_2) + 1/2\alpha_4(t) n_{\text{C}_3\text{S}}(\text{start})\Delta\text{H}_4' \tag{12}$$

Fig. 8 shows the synchrotron X-ray diffraction compared to the calorimetric data by Eqs. (7), (10) and (12). α_4 at the end of the X-ray experiment was calculated to 0.68. By fitting the expression for Q_4 further to the calorimetric data, Reaction 4 was found to reach its end during the first 24 hours of hydration. This is an estimate taking into consideration the approximation of the cements as CA and C_3S, but it nevertheless indicates that the reactions in the paste are fast and that the major part of the Portland cement associated hydration reactions are completed early.

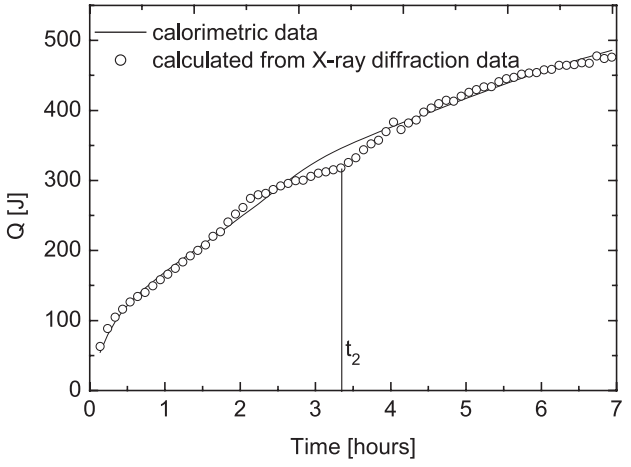

Fig. 8. Accumulated heat calculated from X-ray diffraction data [17] and Eqs. (7), (10) and (12) and measured by calorimeter for paste 1 (100 wt.% β-hemihydrate).

3.3.5. Paste 5

Based on the previously calculated enthalpy of formation of the C–S–H gel and the reactions for paste 1, Reaction 6 was suggested as possible for the ettringite formation in paste 5. It is similar to Reactions 2 and 3, with anhydrite instead of β-hemihydrate and gypsum. Basing the reaction enthalpy and reaction rate for Reaction 6 on the ettringite formation, the accumulated heat from the reaction can be calculated from X-ray diffraction data according to Eq. (13).

$$\text{Reaction6}\quad 104/3\text{H} + \text{CA} + 3\text{C}\hat{\text{S}} + 4/3\text{C}_3\text{S} \rightarrow \text{C}_6\text{A}\hat{\text{S}}_3\text{H}_{32} + 2/3\text{C}_3\text{S}_2\text{H}_4$$

$$Q_6(t) = 1/3\alpha_6(t) n_{\text{C}\bar{\text{S}}}(\text{start})\Delta\text{H}_6 \tag{13}$$

Fig. 9 shows the calculated accumulated heat according to Eq. (13) and the measured accumulated heat from calorimetry. The shape of the measured hydration heat coincides well with the calculated one up to 6 hours of

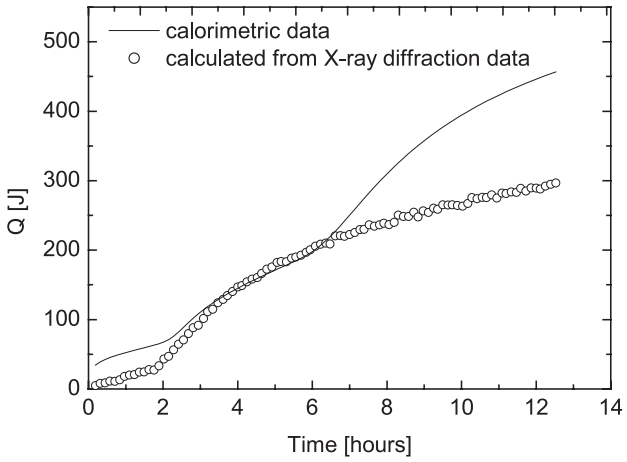

Fig. 9. Accumulated heat calculated from X-ray data diffraction data and Eq. (13) and measured by calorimeter for paste 5 (100 wt.% anhydrite).

hydration were an additional reaction appears to start. In Fig. 9, the calculated hydration heat has $\alpha_6(t \approx 12 \text{ hours})=1$, which means that the ettringite formation is close to completion and the major part of the sulfate is incorporated in ettringite. The difference between the heat produced from ettringite formation and the total produced heat at 12 hours adds up to approximately 150 J. If this heat should come from monosulfate formation, it would incorporate 1/3 of the sulfate available from anhydrite, an amount which is not consistent with the ettringite formation consuming close to all the sulfate. In paste 1, C_2AH_8 was found when all the available sulfate was bound in ettringite. It is a probable hydration product even in paste 5, but no other crystalline hydration product besides ettringite was identified, so the hydration product in the second reaction must be X-ray amorphous or present in a too small amount to be detected by X-ray diffraction.

3.4. Dilatation

Fig. 10 shows the dilatation for the studied pastes. Paste 1 shows expansive properties which coincides in time with the last period of gypsum consumption and resulting ettringite formation [17]. Paste 5 does not show any expansion, rather a very small shrinkage between 3 and 5 hours of hydration. When 25 wt.% of the β-hemihydrate is replaced by anhydrite (paste 2), the expansion is reduced to less than 50% of the one in paste 1. When 50 wt.% is replaced, the paste shows almost no expansion (paste 3). Paste 4 shows a very small expansion at the same scale as paste 3, but while pastes 1–3 all start their expansion at the same time in the hydration process (after approximately 1.5 hours), paste 4 starts much earlier, after less than 1 hour.

When paste 1 hydrates, gypsum forms immediately and forms a solid network in the paste, binding it together. After 30 min of hydration, the paste is filled with gypsum crystals and the cement grains are coated with very small ettringite crystals (Fig. 11a). When ettringite forms and consumes gypsum, larger crystals of ettringite form on the surface of the cement grains (Fig. 11b). They are approximately 5 μm long and grow radially on the cement grains forming small spherulites of ettringite crystals. During the gypsum consumption, the ettringite spherulites have grown to a size were they interact with each other. During the last period of this crystal growth, the paste expands. These results coincide well with the crystal growth theory [2–4] where it was shown that the paste would expand when the spheres with ettringite crystals came in contact with each other. Looking closer at an ettringite spherulite (Fig. 12), it can be seen that it consists of two layers. The inner layer, closest to the cement grain, appears dense or consisting of microcrystalline crystals or a gel and the thickness is a few micrometers. This is probably the small crystal seen on the cement grains in the sample hydrated for 30 min, and because they are detected by X-ray diffraction, it is not a gel. It may also incorporate the C–S–H gel. They are neither sufficiently small to give peak broadening in X-ray diffraction. Outside the dense layer, the larger ettringite crystals have grown. If the inner, dense layer consists of small crystals, there are possibilities for the expansion to be a combination of crystal growth [1–4] and swelling [5,6] as proposed by Deng and Tang [7]. From Fig. 13, it can be seen that the microstructure in paste 5 (100 wt.% anhydrite) is very different from the one in paste 1. The ettringite crystals are much longer, 15–20 μm, and they appear to grow one by one from solution, not on any surface. In this case, crystallisation does not give rise to expansion (Fig. 10). In paste 1, the gypsum formation will solidify the paste very quickly, while in paste 5, the solidification on the paste will dependent on the formation of ettringite, C–S–H gel and other eventual hydration products. When crystals are growing in a paste without a solid matrix, they can move if they get in contact with another crystal and thus grow without strain. As a consequence, they become longer and they will not give rise to expansion. Assuming that the amount of ettringite necessary for the spheres of ettringite to interact and give expansion is constant, i.e., ettringite formed from 50 wt.%

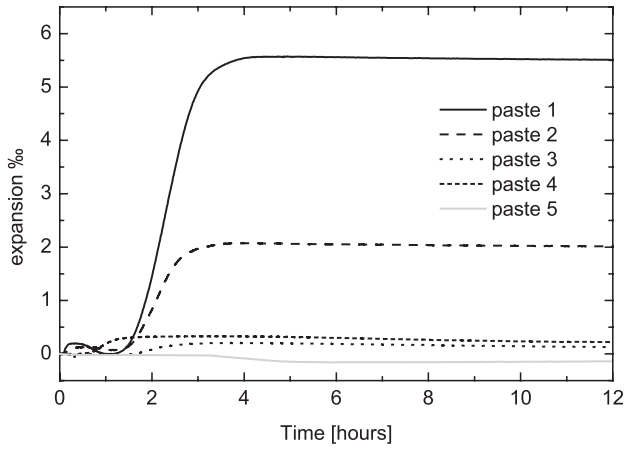

Fig. 10. Dilatation for the studied pastes, average of three measurements.

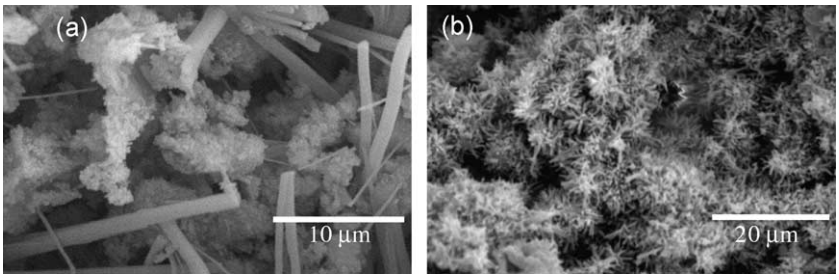

Fig. 11. SEM picture of the microstructure of paste 1 hydrated for (a) 30 min; the paste contains long gypsum crystals and the cement grains are coated with very small crystals of ettringite. (b) For 6 hours; the ettringite crystals are around 5 μm long and grow radially on cement grains, forming spherulites.

β-hemihydrate [17] (Figs. 1 and 10), more β-hemihydrate than 50 wt.% will give expansion. When the amount of hemihydrate is reduced from 100 to 75 wt.%, the expansive fraction (which exceeds 50 wt.%) is halved. The expansion is reduced by more than 50% (Fig. 10), which further supports the crystal growth theory [2–4]. The nucleation during the ettringite growth from β-hemihydrate in the mixes (pastes 2 and 3) was increased compared to paste 1 (Table 2). This can be caused by dissolution of anhydrite, or gypsum contaminating anhydrite, which contributes to the formation of ettringite nuclei. If the ettringite formed from β-hemihydrate crystallises on these nuclei, they will probably not contribute to expansion because they are not on the surface of the cement grains, but in solution. This may explain why the expansion was reduced by more than 50% in paste 2 compared to paste 1. The ettringite formed from anhydrite dissolution does not contribute to expansion; consequently. it cannot continue to grow on the ettringite formed during hemihydrate and gypsum dissolution. This further supports the theory that the two reactions are independent. Pastes 3 and 4 show minor expansions despite insufficient β-hemihydrate according to the crystal growth theory. This shows that it is likely that a small amount of swelling expansion does occur at high relative humidity.

4. Conclusions

(i) The kinetics of ettringite formation is very dependent on the source of the calcium sulfate. When β-hemihydrate and anhydrite are mixed, the ettringite formation rate can be described by addition of the kinetic expressions of the two pure pastes, with only β-hemihydrate and anhydrite, with alteration of the kinetic parameters, down to 50 wt.% β-hemihydrate. With 25 wt.% β-hemihydrate, the ettringite formation appears to be changed.

(ii) The results from synchrotron X-ray diffraction and calorimetry coincide well for paste 1 (100 wt.% β-hemihydrate). A series of reactions has been proposed and appear to give a good description of the hydration reactions in the paste implying that there are no major hydration products that are not detected by X-ray diffraction. For paste 5 (100 wt.% anhydrite), the two experimental methods appear to coincide well in shape up to 6 hours of hydration when a second reaction, parallel to the formation of ettringite, starts. The hydration product is unlikely to be monosulfate and is not detected by X-ray diffraction.

(iii) Ettringite in paste 1 appears to grow in two stages: first, a layer of small crystals cover the cement grains, then larger crystals grow radially on the grains. The expansion is caused by contact between the growing ettringite crystal spherulites. This may be in combination with swelling of an inner ettringite layer. In paste 5, the ettringite crystals do not grow on the surface of the cement grains, but arbitrarily from solution, and they do not give rise to expansion. In the mixes, only the ettringite formed from β-hemihydrate

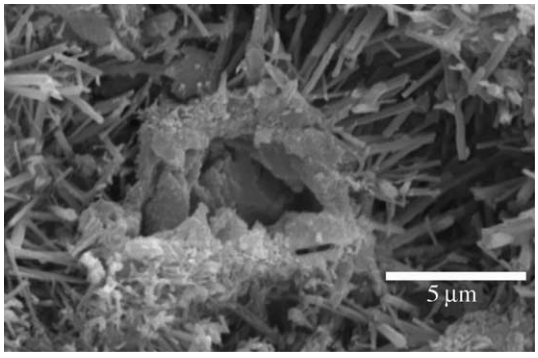

Fig. 12. The hydration products around a not fully hydrated cement grain in paste 1 after 24 hours of hydration. The inner shell is dense and outside the shell ettringite crystals grow radially.

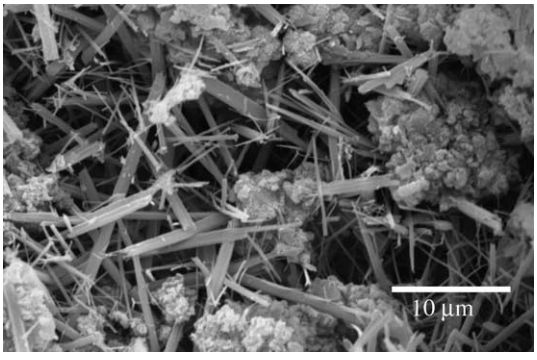

Fig. 13. SEM picture of the microstructure of paste 5 hydrated for 5 hours. The ettringite needles are 15–20 μm long and grow arbitrarily. After 12 and 24 hours, the microstructure is very similar to that after 5 hours of hydration.

gives expansion and a β-hemihydrate content over 50 wt.% of the calcium sulfate is necessary to get expansion by crystal growth. These results support the crystal growth theory.

Acknowledgement

Financial support from the Swedish Natural Research Council (NFR) and the Scancem Research and Development Fund is gratefully acknowledged. We would like to thank Åke Oskarsson, Yngve Cerenius and Thomas Ursby for help in connection with the collection of X-ray diffraction data and Lars Wadsö for providing the calorimeter.

References

[1] M.D. Cohen, Theories of expansion in sulfoaluminate-type expansive cements: schools of thought, Cem. Concr. Res. 13 (6) (1983) 809–818.
[2] K. Ogawa, D.M. Roy, $C_4A_3\hat{S}$ hydration, ettringite formation, and its expansion mechanism: II. Microstructural observation of expansion, Cem. Concr. Res. 12 (1) (1982) 101–109.
[3] M. Ish-Shalom, A. Bentur, Properties of type K expansive cement of pure components: I. Hydration of unrestrained paste of the pure expansive component, Cem. Concr. Res. 4 (4) (1974) 519–532.
[4] A. Bentur, M. Ish-Shalom, Properties of type K expansive cement of pure components: II. Proposed mechanism of ettringite formation and expansion in an unrestrained paste of the pure expansive component, Cem. Concr. Res. 4 (5) (1974) 709–721.
[5] P.K. Mehta, Mechanism of expansion associated with ettringite formation, Cem. Concr. Res. 3 (1) (1973) 1–21.
[6] P.K. Mehta, S. Wang, Expansion of ettringite by water adsorption, Cem. Concr. Res. 12 (1) (1982) 121–122.
[7] M. Deng, M. Tang, Formation and expansion of ettringite crystals, Cem. Concr. Res. 24 (1) (1994) 119–126.
[8] P.W. Brown, P. LaCroix, The kinetics of ettringite formation, Cem. Concr. Res. 19 (6) (1989) 879–884.
[9] P. Norby, Hydrothermal conversion of zeolites: an in situ synchrotron X-ray powder diffraction study, J. Am. Chem. Soc. 119 (1997) 5215–5221.
[10] P. Norby, J.C. Hanson, A.N. Fitch, G. Vaughan, L. Flaks, A. Gualtieri, Formation of α-Eucryptite, $LiAlSiO_4$: an in-situ synchrotron X-ray powder diffraction study of a high temperature hydrothermal synthesis, Chem. Mater. 12 (2002) 1473–1479.
[11] R.H. Doremus, Rates of Phase Transformation, Academic Press, London, 1985.
[12] A.F. Gualtieri, Synthesis of sodium zeolites from a natural halloysite, Phys. Chem. Miner. 28 (2001) 719–728.
[13] I. Odler, J. Colán-Subauste, Investigation on cement expansion associated with ettringite formation, Cem. Concr. Res. 29 (5) (1999) 731–735.
[14] P.K. Mehta, G. Lesnikoff, Hydration characteristics and properties of shrinkage-compensating cements, Proc. 6th Intl. Congr. Chem. Cem. (3) (1976) 89–105.
[15] L. Amathieu, T.A. Bier, K.L. Scrivener, Mechanisms of set acceleration of portland cement through CAC addition, in: R.J. Mangabhai, F.P. Glasser (Eds.), Calcium Aluminate Cements 2001, IOM Communications, London, 2001, pp. 303–315.
[16] J.P. Bayoux, A. Bonin, S. Marcdargent, Study of the hydration properties of aluminous cement and calcium sulfate mixes, in: R.J. Mangabhai (Ed.), Calcium Aluminate Cement, E&FN Spoon, London, 1990, pp. 320–334.
[17] C. Evju, S. Hansen, Expansive properties of ettringite in a mixture of calcium aluminate cement, Portland cement and β-calcium sulfate hemihydrate, Cem. Concr. Res. 31 (1) (2001) 257–261.
[18] C. Evju, Initial hydration of cementitious systems using a simple isothermal calorimeter and dynamic correction, J. Therm. Anal. Calorim. 71 (3) (2003) 829–840.
[19] H.F.W. Taylor, Cement Chemistry, Academic Press, London, 1990.
[20] Ping Gu, J.J. Beaudoin, E.G. Quinn, R.E. Myers, Early strength development and hydration of ordinary Portland cement/calcium aluminate cement pastes, Adv. Cem. Based Mater. 6 (1997) 53–58.
[21] P. Garcés, E. Garcia Alcocel, C. Garcia Andreu, Hydration characteristics of high alumina cement/Portland cement mixtures, ZKG Int. 11 (1998) 646–649.
[22] C. Solberg, S. Hansen, Dissolution of $CaSO_4 \cdot 1/2H_2O$ and precipitation of $CaSO_4 \cdot 2H_2O$. A kinetic study by synchrotron X-ray diffraction, Cem. Concr. Res. 31 (4) (2001) 641–646.
[23] J.E. Macintyre (Ed.), Dictionary of Inorganic Compounds, vol. I, Chapman and Hall, London, 1992.
[24] G.H. Aylward, T.J.V. Findlay (Eds.), SI Chemical Data, 4th edition, John Wiley and Sons Australia, Brisbane, 1998.
[25] V.I. Babushkin, G.M. Matveyev, O.P. Mchedlov-Petrossyan, Thermodynamics of Silicates, Springer-Verlag, Berlin, 1985.